Magazine of Civil Engineering. 2019. 90(6). Pp. 47–61
Инженерно-строительный журнал. 2019. № 6(90). С. 47–61

Magazine of Civil Engineering

ISSN 2071-0305

journal homepage: http://engstroy.spbstu.ru/

DOI: 10.18720/MCE.90.5

Risk of surface blast load on pile foundations

***Y.E-H. Ibrahim*[a,b]*, M. Nabil*[b]*,**
[a] *Prince Sultan University, Riyadh, Saudi Arabia*
[b] *Zagazig University, Zagazig, Egypt*
** E-mail: yibrahim@vt.edu*

Keywords: soil, buildings, blast load, finite element, pile foundation, expanded polystyrene

Abstract. Recent terrorist attacked has raised the importance of studying the structural response under blast loads. Most of the past research has focused on the superstructure performance without considering the foundation behavior under blast loads. In this research, a pile foundation system was analyzed using detailed finite element analysis using ABAQUS under blast load to investigate the effectiveness of different mitigation techniques. The foundation system includes nine concrete piles encased in steel pipes with external diameters of 0.6 m. The piles have a length of 20 m in silty clay and stiff clay layers. The piles are connected using a reinforced concrete raft with dimensions of 10 m×10 m and a thickness of 1 m. The blast load considered resulted from a surface explosive charge of 457 kg of TNT at a standoff distance 2.5 m from raft and at a height of 0.56 m above ground surface. The raft was loaded by 200 kN/m2 to represent the load transferred from the structure. Barrier walls from different materials including aluminum, rubber, Thermoplastic polyurethane (TPU) and Expanded Polystyrene (EPS) were considered to mitigate the blast load effect on the pile foundation. Also, an open trench before the raft was considered and compared to the used wall barriers. It was observed that the open trench and a wall barrier from Expanded Polystyrene showed the best mitigation to the blast effect compared to the original case and other wall barriers from different materials. A parametric study was conducted to optimize the selected EPS wall barrier in terms of thickness and depth.

1. Introduction

After the recent attacks on many iconic buildings, many researchers have focused in their research on the structural response of buildings when subjected to blast loads and possible solutions to mitigate the risk of this threat [1–6]. Due to the complexity of the problem and the severe damage occurring in the superstructures, most of the research conducted in this area focused on the analysis and response of the superstructure without taking in consideration the effect of the foundation. Dynamic waves resulting from surface blast explosions can severely damage the foundation and underground structures through dynamic loads exerted from reflected waves after hitting the ground [7–9].

Most of the research work addressing the soil and structural response of foundations and underground structures under blast loads was conducted through finite element analysis using powerful packages such as ABAQUS [10], LS-Dyna [11] and ANSYS [12] to consider the nonlinearity of materials, soil block modeling with its boundary conditions and dynamic loads exerted on soil and underground structures and foundations [13–18]. The finite element analysis provides well representation of the problem without the need for experimental work, which is hard to perform and this explains the limited research work in this area [19–20].

Representing the blast loads in the finite element analysis needs careful consideration in order to obtain accurate results and real simulation. Based on spherical explosive charges, most of empirical equations were developed in order to calculate the pressure that is generated by air, surface, subsurface or under water explosives on structures [7–9, 21–26]. The calculated pressure exerted by blast loads through these empirical equations is affected by different parameters such as the weight of explosive charge, its duration, time of wave

Ibrahim, Y.E-H., Nabil, M. Risk of surface blast load on pile foundations. Magazine of Civil Engineering. 2019. 90(6). Pp. 47–61. DOI: 10.18720/MCE.90.5

Ибрагим Я, Набил М. Риск внешней взрывной нагрузки на свайные фундаменты // Инженерно-строительный журнал. 2019. № 6(90). С. 47–61. DOI: 10.18720/MCE.90.5

arrival at the structure and particle displacement, velocity, and acceleration. The pressure generated on soils depends on soil properties such as void ratio and water content, especially in cohesive soils compared to granular soils with high relative density [21, 26].

The shape of the crater developed in soils due to blast explosions is significantly affected by the weight of explosive charge. Explosives with higher weights lead to significant increase in energy dissipation. Pile foundations subjected to surface blast loads may not be used to support superstructure after the blast because of the high horizontal stresses developed in the top portions of piles close to the explosive charge [27].

Many researchers investigated ways to mitigate the risk of blast loads on underground structures using barriers. The studied solutions included using barriers from different materials between the surface explosion and the underground structure as well as using trenches filled with polystyrene foam. It was concluded that these solutions had great influence on reducing the blast risk on underground structures especially using compressible geofoam barrier made of polyurethane [28–31].

In this research, the effectiveness of using different techniques to mitigate the blast load effect on pile foundation and surrounding soil was investigated using detailed finite element analysis using ABAQUS. The pile foundation includes nine piles connected with a raft foundation. The mitigation techniques included the using open trench or wall barrier from different materials such as aluminum, rubber, thermoplastic polyurethane (TPU) and expanded polystyrene (EPS). The blast load effect was considered through an explosive charge of 457 kg of TNT placed at a standoff distance of 2.5 m from the edge of the raft and at a height of 0.56 m above ground surface. All barrier walls are assumed to have 0.25 m thickness and placed at the edge of the raft foundation. The walls extended to 5.0 m below the ground surface. After comparing the effectiveness of using these techniques, a parametric study was conducted to optimize the use of the most effective mitigation technique in order to obtain the best protection of the pile foundation under blast load.

2. Methods

First, in order to verify the representation of blast load on soil block and its effect on the formation of the soil crater in terms of its radius and depth, a soil model was created using ABAQUS with its CONWEP representation of blast load. The results were compared to that obtained from previous empirical equations provided by Cooper [9] and Gould [32] and previous finite element model [33]. The developed finite element model is shown in Figure (1.a). The soil block had the dimensions of 100 m×100 m×50 m and 10 m of non-reflected boundaries in both X and Y directions and used a fixed boundary in Z direction. A 100-kg spherical charge with a density of 1630 kg/m^3 was used. The scale distance R from the surface of the earth to the center of the charge was 0.50 m to confirm that the CONWEP will work well with the target surface X-Y surface.

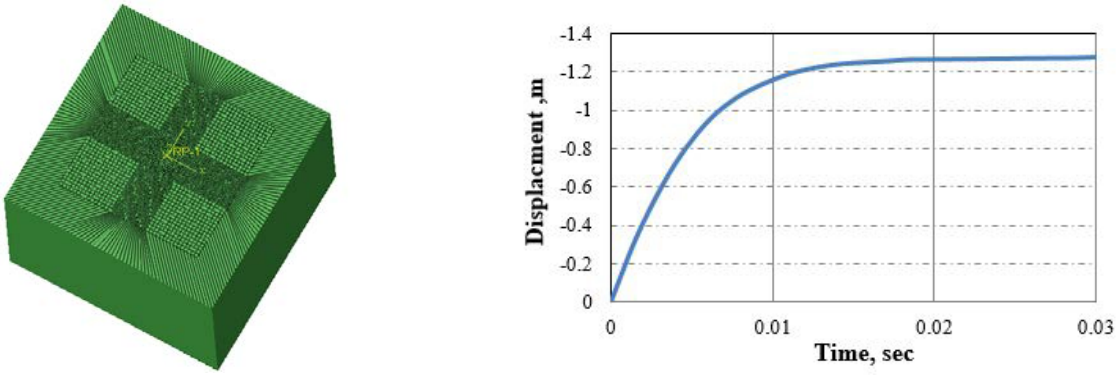

a) Finite Element Model b) Time history of vertical displacement at center of crater

Figure 1. Finite element model of soil block used for verification.

An elastic–plastic analysis using the Drucker-Prager Cap model was conducted. The apparent crater radius and depth, which were measured relative to the original surface, were compared to the empirical equations and previous finite element model (Table 1). Figure 1.b shows the time history of the vertical displacement of the center of crater after the soil block was subjected to the blast load.

Table 1. Crater depth and width from numerical analysis, empirical equations.

Method	Apparent Crater Radius (m)	Apparent Crater Depth (m)
Cooper [9]	1.80	–
Gould [32]	2.85	1.19
Previous Finite Element Model [33]	1.37	1.20
Developed Finite Element Model	1.69	1.27

According to the results obtained, the developed finite element model provided results with acceptable accuracy in terms of the radius and depth of the soil crater. Accordingly the finite element model was used in this research.

The pile foundation considered in this study consisted of 9 reinforced concrete piles with a diameter of 600 mm each encased in 15 mm thick steel casing with a total length of 20 m. The piles are 4.2 m (center to center) apart from each other. The piles are connected with a raft foundation with the dimensions of 10 m×10 m with a total thickness of 1.0 m. A uniform load with an intensity of 200 kN/m^2 was applied on the raft to represent the load transferred from the structure. Blast charge of 457 kg of TNT was placed at a standoff distance 2.5 m from closest raft edge and at a height of 0.56 m above ground surface. The soil block considered had the dimensions of 100 m x 100 m in plan with a depth of 50 m. Standard elements were used for soil block surrounding the raft and pile foundations followed by infinite elements in order to provide quiet boundary conditions to the finite element model. The soil profile consisted of upper layer of silty clay with a total thickness of 10 m. This layer was followed by 40-m thick stiff clay. The soil properties are given in the following Table 2 [34]:

Table 2. Properties of soil layers [34].

Soil Property	silty clay	stiff clay
Young's Modulus (MPa)	51.7	328
Poisson Ratio	0.45	0.17
Density kg/m3	1920	1920
Material Cohesion (MPa)	0.036	1.38
Material angle of friction (degrees)	24	36.9
Cap eccentricity parameter	0.3	0.33
Initial cap yield surface position	0.02	0.02
Transition surface radius parameter	0.05	0.01
Cap hardening behavior [Stress (MPa), plastic volumetric strain]	[2.75, 0] [4.83, 0.02] [5.15, 0.04] [6.20, 0.08]	[2.75, 0] [4.14, 0.02] [5.51, 0.05] [6.20, 0.09]

A wall barrier was used at closer edge of the raft with a length equals to the length of the raft (10.0 m). The depth of wall barrier was 5.0 m with its top at the ground surface. The thickness of the wall was 0.25 m. Figure 2 shows the arrangement of the piles, wall location and blast charge position.

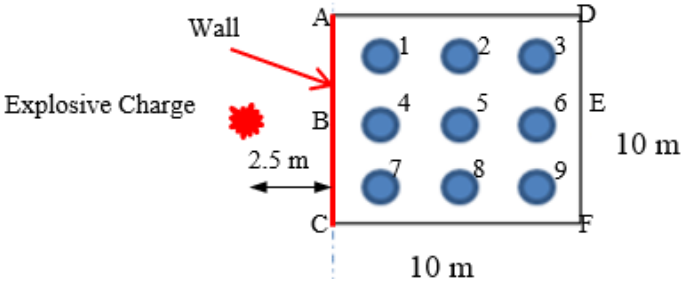

Figure 2. Pile foundation arrangement and wall location.

Different types of wall barriers were considered including:

- No barrier (original case)
- Open trench
- Barrier from different materials (Aluminum, Thermoplastic polyurethane TPU, Rubber and Expanded Polystyrene EPS)

Table 3 shows the different physical properties of materials used.

Table 3. Different physical properties of materials used.

Material	Modulus of Elasticity E (MPa)	Poisson Ratio ν	Specific Weight γ (kN/m^3)
Aluminum	73.09 * 10^3	0.33	27.4
Thermoplastic polyurethane (TPU)	158	0.40	11.5
Rubber	76.53	0.45	1.1
Expanded Polystyrene (EPS)	7.5	0.00	1.0

Soil block was modeled in ABAQUS using Lagrangian three-dimensional solid continuum elements. ABAQUS CONWEP empirical model was used to model the blast load on soil and foundations through defining the equivalent TNT explosive charge and its location. The objective of the analysis was to consider the soil behavior including crater formation and pile foundation performance [33]. In order to represent the soil behavior, Drucker-Prager Cap model in ABAQUS was used. This model considers soil hardening/softening and stress path dependence [35]. CIN3D8 elements were used to model the infinite elements and the boundary conditions of the considered soil block. These elements are 3D 8-nodes solid continuum finite elements. C3D8R elements were used to model the concrete elements of raft and piles. These elements are 8-node solid elements with reduced integration. In order to model the inelastic behavior of concrete material of raft and piles, concrete damage plasticity model was used. This model considers the concept of isotropic damaged elasticity in combination with isotropic tensile and compressive plasticity. Based on the material properties of Chopra and Chakrabarti [36], stress-strain curve was developed by Martin [37], which was used in this study. Values of yielding and failure strains of concrete were 0.002 and 0.004, respectively. In order to model the plasticity in ABAQUS, true stress and logarithmic plastic strain were used. Figure 3 shows the finite element model of the soil and pile foundation.

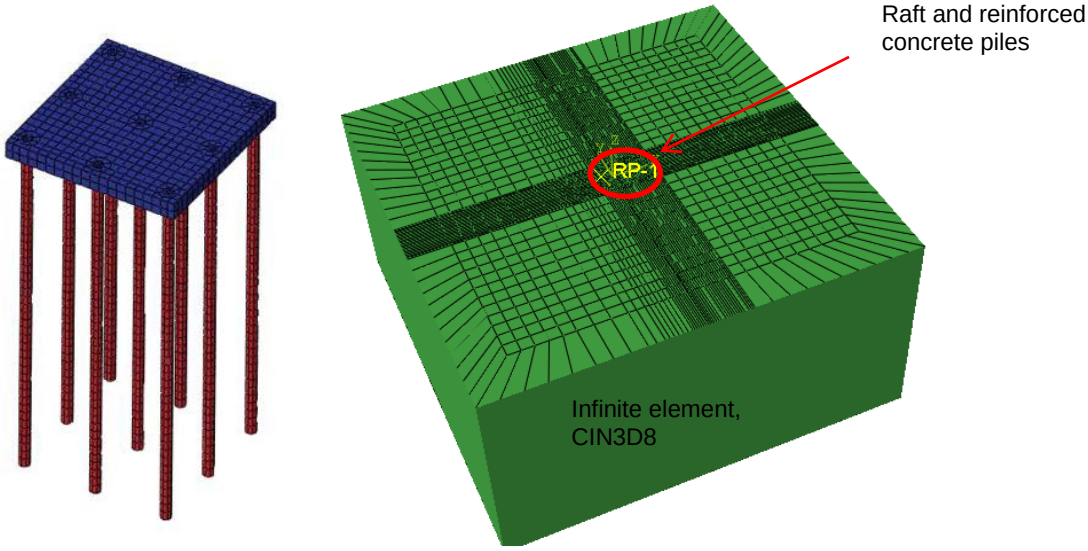

a) Raft and piles b) Whole finite element model

Figure 3. Finite element model of pile foundation and soil block.

Aluminum is modeled using Johnson-Cook constitutive model [38], which provides simple mathematical relationship of stress-strain-temperature using material parameters; A, B, C and m as shown in Table 4.

Table 4. Johnson-Cook parameters for Aluminum [38]

A (MPa)	B (MPa)	C	M
349	426	0.0083	1

Ductile failure criterion in ABAQUS was used to model TPU. The parameters needed to model the isotropic hardening are given in Table 5 [38]

Table 5. Isotropic hardening stress-strain values for TPU [39]

Yield stress (MPa)	11.05	25.92	45.36	119.02	265.26	295.43	390.17
Plastic strain	0	0.36	0.76	1.42	1.90	2.18	2.97

The strain rate of TPU, fracture strain for ductile damage and Stress triaxiality were assumed to be 0.001 S^{-1}, 2.9 and 0.33, respectively [39].

Hyperelastic and viscoelastic properties of rubber were modeled using ABAQUS. Neo-Hookean model for hyperelastic behavior was used. The material constants C_{10}, C_{01} and D_1 were 1 MPa, 0 and 5.085 * 10^{-3} Pa, respectively. Prony series was used to model the viscoelastic behavior of the rubber. The material constants used were g_i, K_i and τ_i with values of 0.3, 0 and 0.1, respectively. These parameters can be obtained from shear or relaxation test [40].

To model the hyperfoam material properties of EPS, ABAQUS default parameters were used to define the strain energy function. The hyperfoam material is different from the regular hyperelastic material in terms of its high compressibility (ABAQUS Manual). Viscoelastic behavior of the material was modeled through

assigning values for the parameters used to define the prony series. The values used for this material were 0.5, 0.5 and 0.003 for g_i, K_i and τ_i, respectively

Note that the dimensions of the barrier wall used were kept the same for all materials during this study, even though it might not be practically accepted. This was decided in order to compare different responses of these materials and to decide on the most effective one. Then the final selected material can be more investigated to get the best enhancement can be obtained for the mitigation of blast load effect considering the cost and availability.

3. Results and Discussions

The finite element analysis of the pile foundations, soil block and wall barrier was conducted under blast load of 457 kg of TNT at a standoff distance 2.5 m from closest raft edge and at a height of 0.56 m above ground surface. The effect of wall barrier used was considered through using different wall materials as well as open trench and comparing the results with the original case, where the pile foundations are not protected. Figures from 3 to 18 show the effect of different wall barrier from different materials and open trench on the response of soil and pile foundation under the effect of blast load.

Figure 4 shows the soil crater developed after the blast in the original case. A typical crater shape was obtained. The maximum vertical downward displacement in soil was 0.75 m at distance of 2.5 m from raft edge. The soil profile was almost not affected at a distance of around 6.0 m from the raft edge in front of the explosion. Figure 4 shows the lateral displacement of the soil for the original case. The maximum lateral displacement was 0.17 m at 3.0 m from the raft edge in front of the explosion.

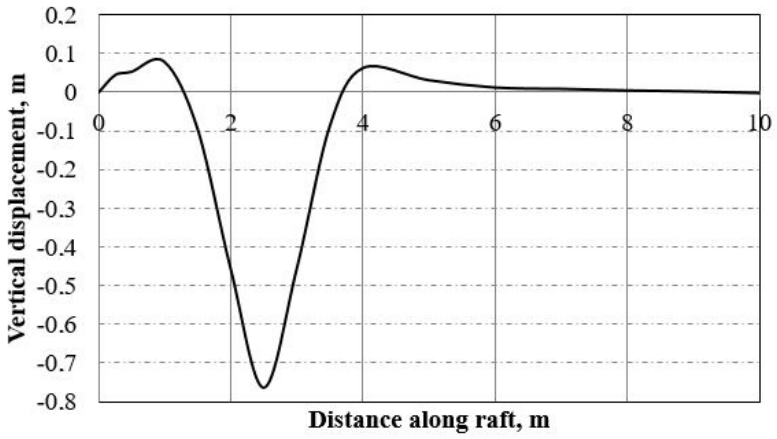

Figure 4. Crater shape (Distance measured from B).

In the first part of the analysis, the wall barrier had a thickness of 0.25 m and a total depth of 5.0 m with its top at the same level with the top level of the raft foundation, which is at the ground surface. Figures 6 and 7 show the vertical and lateral displacement at the middle axis of the raft foundation (line BE) for different cases considered. The maximum vertical displacement at the original case was 0.6 cm at point B. Using open trench resulted in much reduction of the vertical displacement to around 0.1 cm, while the wall barrier resulted in reduction of the value in most of the cases. Similarly, the lateral displacement of the middle axis of the raft was around 0.9 cm at point B at the original case and it was reduced significantly upon using the open trench to around 0.1 cm. EPS wall barrier resulted in considerable reduction of the lateral displacement to around 0.36 cm, and the EPS wall barrier was considered the best barrier used, in this regard.

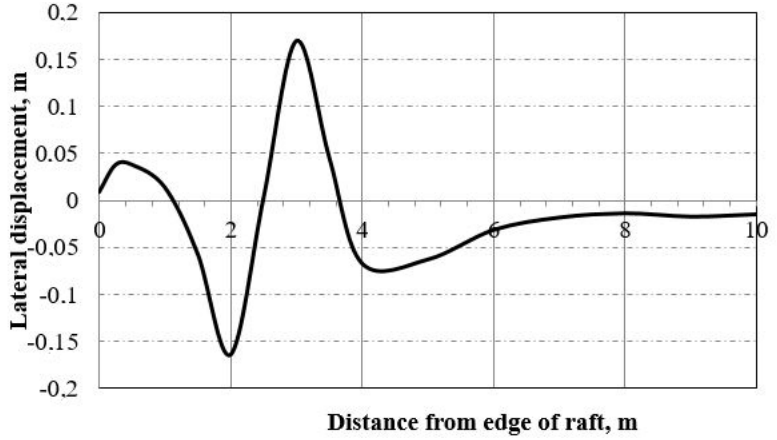

Figure 5. Lateral displacement in the soil (Distance measured from B).

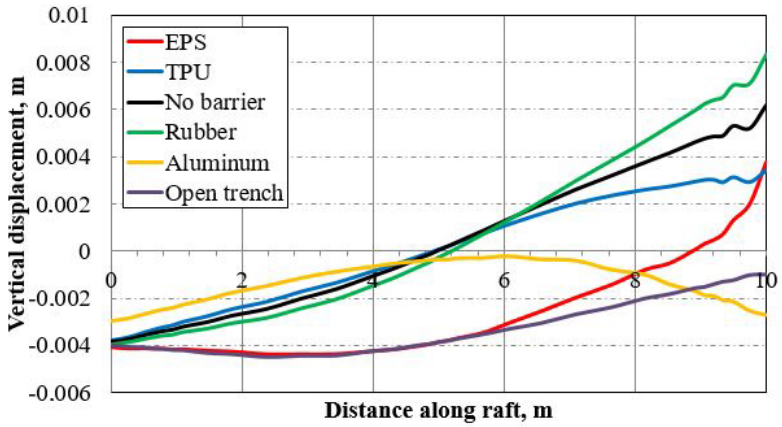

Figure 6. Vertical displacement at raft foundation (E at zero and B at 10 m) at *t* = 0.03 seconds.

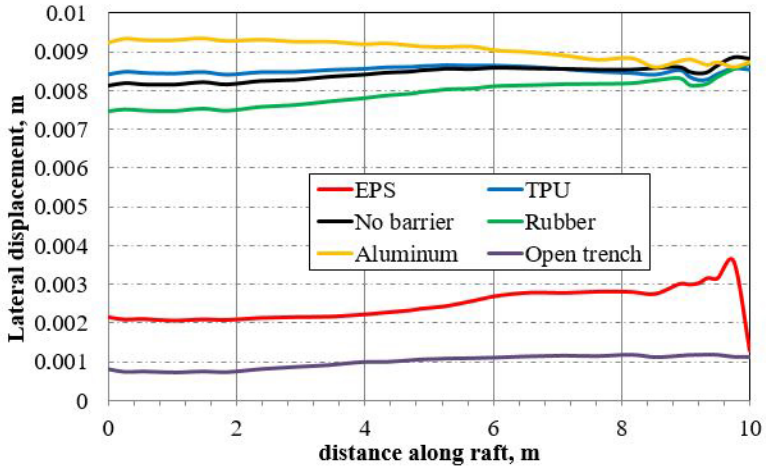

Figure 7. Lateral displacement at raft foundation (E at zero and B at 10 m) at *t* = 0.03 seconds.

Figure 8 shows the deformation of the set of piles due to the blast load in the original case. It is clear that the most deformed pile was the pile close to the explosive charge (number 4) and the large deformations occurred at the top part of the piles. Figure 9 to Figure 13 show the response of the edge pile (pile number 4); while Figure 14 to Figure 19 show the response of the central pile (pile number 5). According to Figure 9, TPU and rubber barriers had no considerable effect on the vertical displacement at the top of the edge pile while the vertical displacement at its top was increased in the case of open trench, EPS and Aluminum barrier wall. The pile foundations experienced the largest residual vertical displacement of the edge pile (0.25 cm) at its top in the Aluminum barrier case. Figures 10 and 11 show the lateral and vertical displacements over the length of the edge pile (number 4) in all cases, respectively.

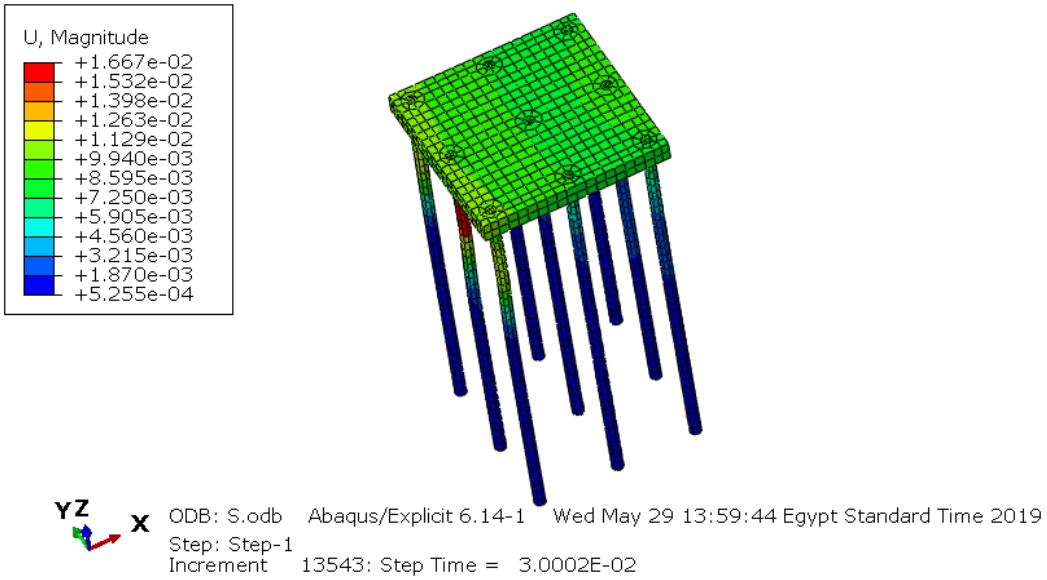

Figure 8. Deformed shape of pile foundation at *t* = 0.03 seconds in the original case (no wall barrier).

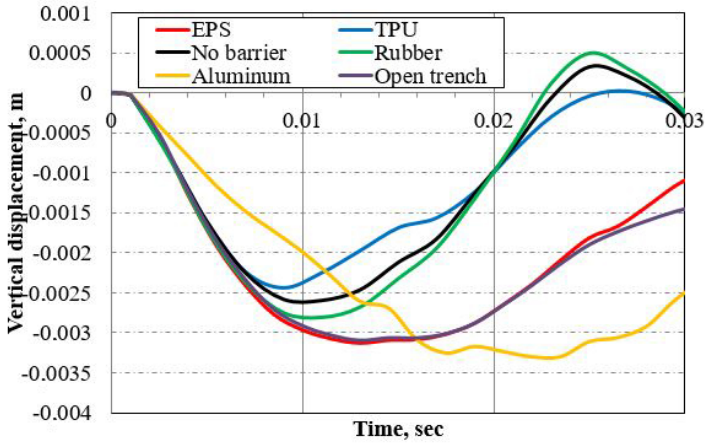

Figure 9. Vertical displacement at central of edge pile (Pile No. 4) at *t* = 0.03 seconds.

The maximum lateral displacement of the pile occurred at depth of 3.0 m in all cases, except for the open trench case, where the maximum lateral displacement was at depth of 5.0 m. Open trench and EPS barrier wall resulted in significant reduction of the lateral displacement, especially in the open trench case, compared to the original case. Rubber barrier wall has no effect on the lateral displacement, while more lateral displacement was obtained when using TPU and Aluminum walls. Similar results were obtained regarding the vertical displacement of the edge pile with the occurrence of maximum downward displacement at depth of 7.0 m for most of the cases and maximum upward displacement at its top as shown in Figure 11.

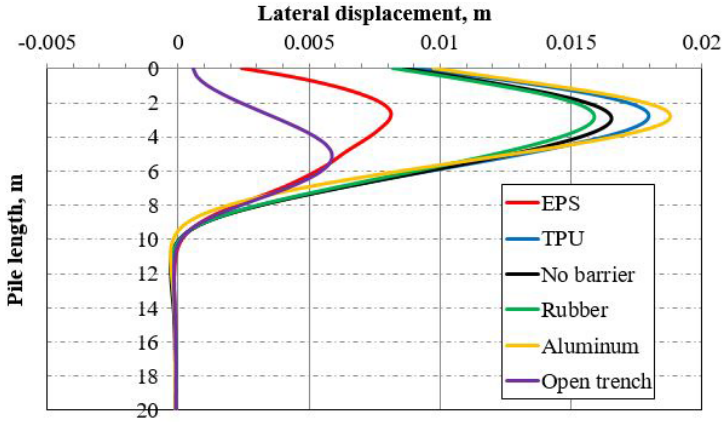

Figure 10. Lateral displacement at edge pile (Pile No. 4) at *t* = 0.03 seconds.

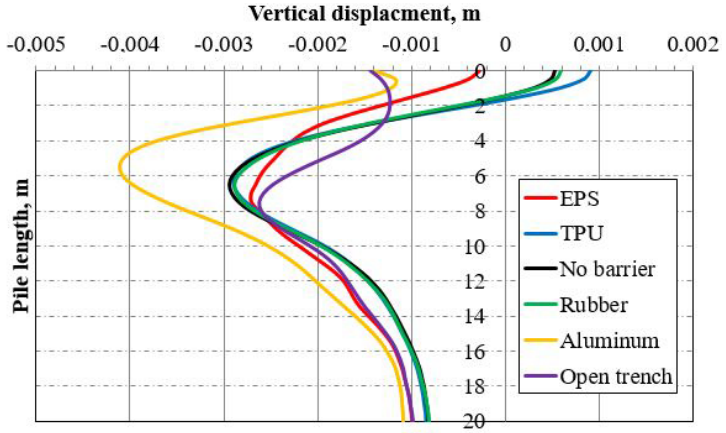

Figure 11. Vertical displacement at edge pile at *t* = 0.03 seconds.

Figures 12 and 13 show the vertical and lateral stresses developed in the pile number 4. Values of vertical stresses did not show big variances in most of the cases, however, the lateral stresses were much reduced in the open trench case. Higher vertical stresses were received in the top part of the edge pile with the maximum vertical stress at depth of 3.0 m from the pile top. The maximum lateral stresses were experienced at the top of the pile with much less stresses in lower parts of the edge pile. The open trench had

better effect on the vertical and lateral displacements and stresses on the edge pile when subjected to blast loads.

Considering pile number 5, which is located under the center of the raft, the lateral and vertical displacement at the top of the pile are shown in Figures 14 and 15. By the end of the blast load duration, significant reduction in lateral displacements was obtained in both cases; open trench and EPS wall barrier.

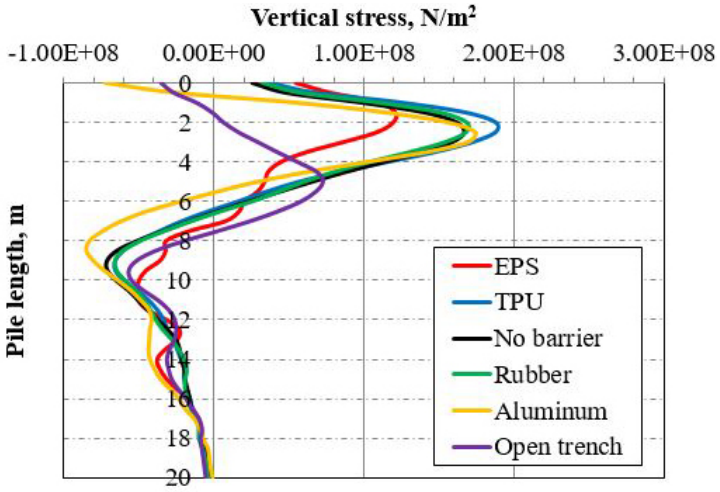

Figure 12. Vertical stress at edge pile (Pile No. 4) at *t* = 0.03 seconds.

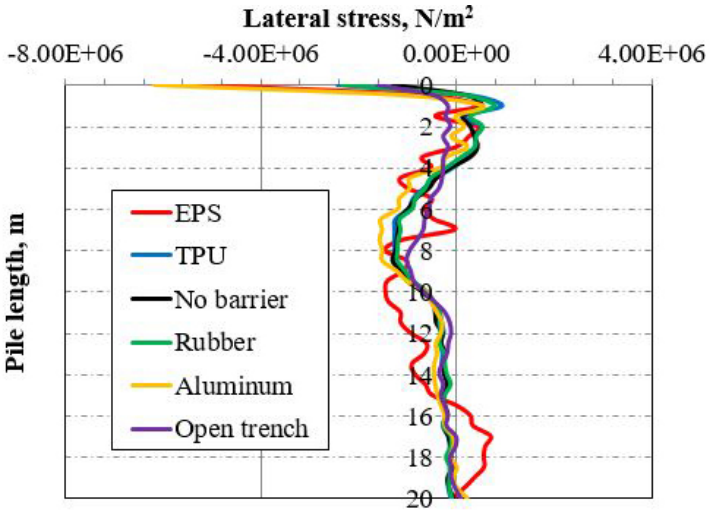

Figure 13. Lateral stress at edge pile (Pile No. 4) at *t* = 0.03 seconds.

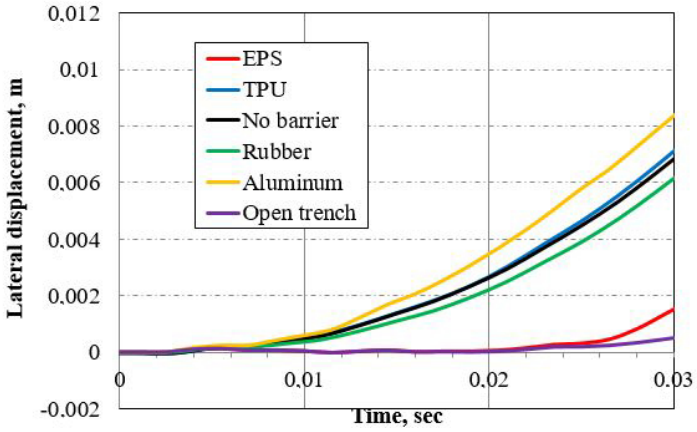

Figure 14. Lateral displacement at central pile (Pile No. 5).

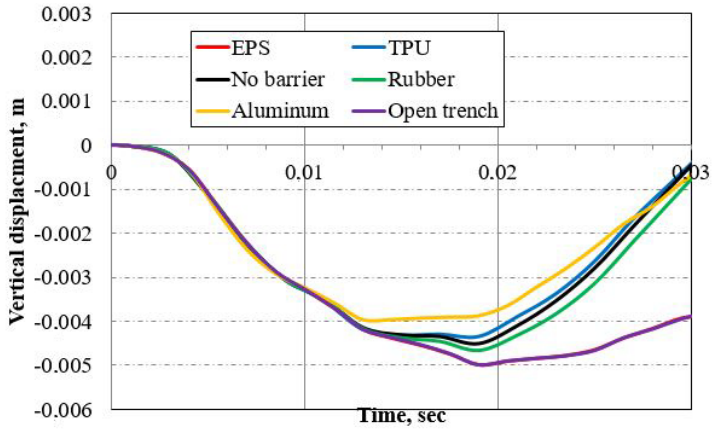

Figure 15. Vertical displacement at central pile (Pile No. 5).

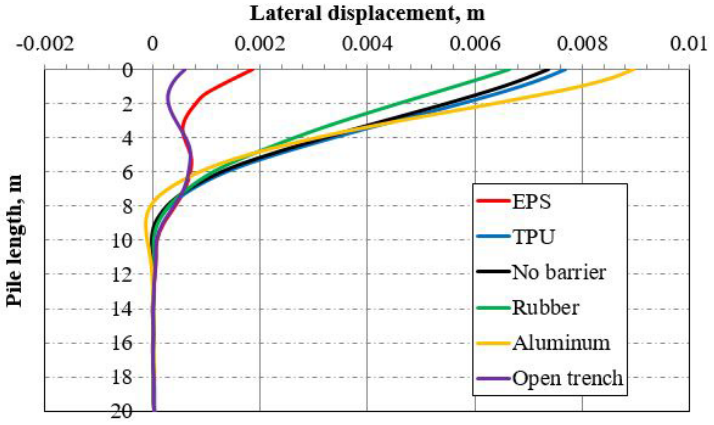

Figure 16. Lateral displacement at center pile (Pile No. 5) at *t* = 0.03 seconds.

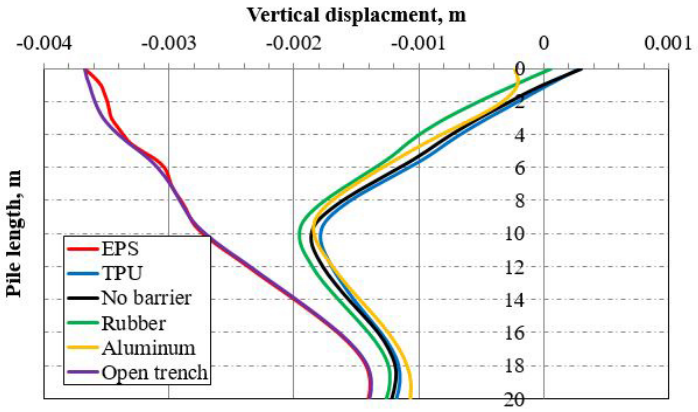

Figure 17. Vertical displacement at center pile (Pile No. 5) at *t* = 0.03 seconds.

After reaching a conclusion that the EPS wall barrier is the best wall barrier in terms of mitigating the blast load risk on the pile foundation, a parametric study was conducted to optimize the effectiveness of this wall barrier in this regard. Three cases were considered to study the effect of the wall thickness of EPS wall barrier including using thickness of 50 cm and 100 cm besides the case considered earlier (25 cm) and comparing these cases with the original case that has no wall barrier. The results of this parametric study are shown in Figures 20 to 27. According to the results, considerable enhancement was obtained upon increasing the wall thickness in terms of the lateral and vertical displacements over the pile length (Figures 20 and 21, respectively for edge pile), time history of lateral and vertical displacement at the top of the central pile (Figures 22 and 23, respectively), lateral displacement over the length of the central pile and finally the vertical displacement along the central X-axis of the raft. The top half of the edge pile experienced large lateral displacements in all cases while no noticeable lateral displacements were spotted in the lower part. The maximum vertical displacements were obtained at a depth of 8 to 10 m in all cases. Increasing the wall barrier thickness from 50 cm to 100 cm has a negligible effect on the enhancement of the pile foundations under blast loads. According to the importance of the building and the possibility of being targeted in a terrorist attack, the designer and the owner may choose the thickness of the wall barrier to mitigate the blast load risk on the foundation. According to the results obtained, the maximum recommended wall barrier thickness is 50 cm.

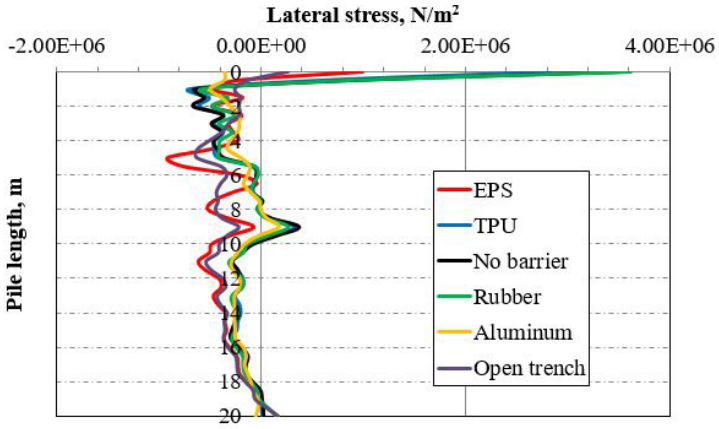

Figure 18. Lateral stress at center pile (Pile No. 5) at *t* = 0.03 seconds.

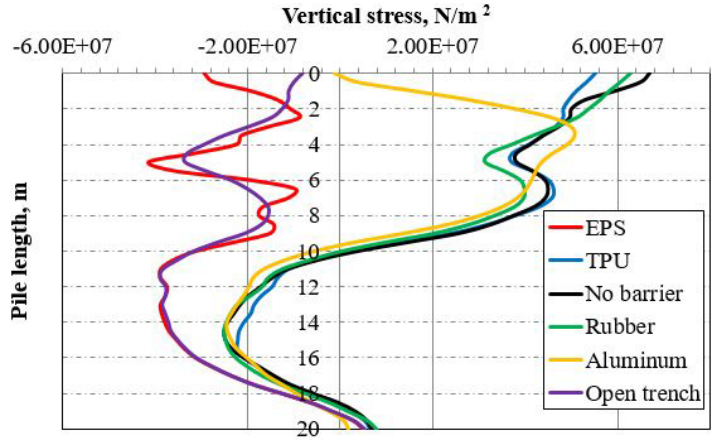

Figure 19. Vertical stress at center pile (Pile No. 5) at *t* = 0.03 seconds.

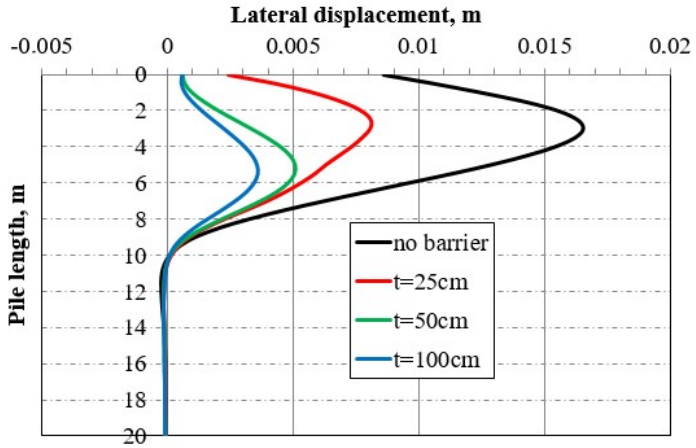

Figure 20. Lateral displacement of Pile No. 4 at *t* = 0.03 seconds.

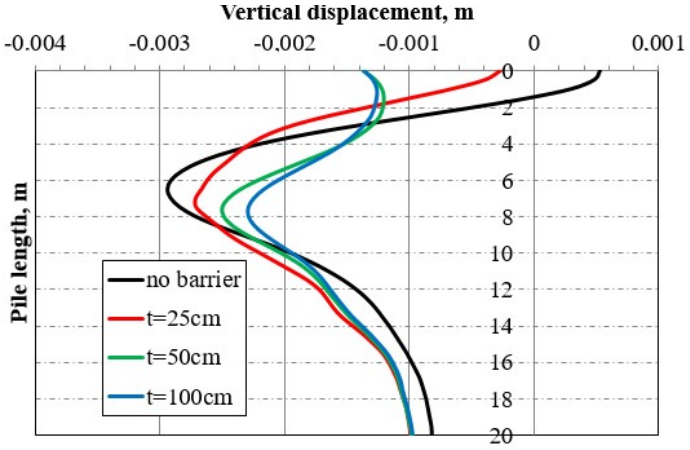

Figure 21. Vertical displacement of Pile No. 4 at *t* = 0.03 seconds.

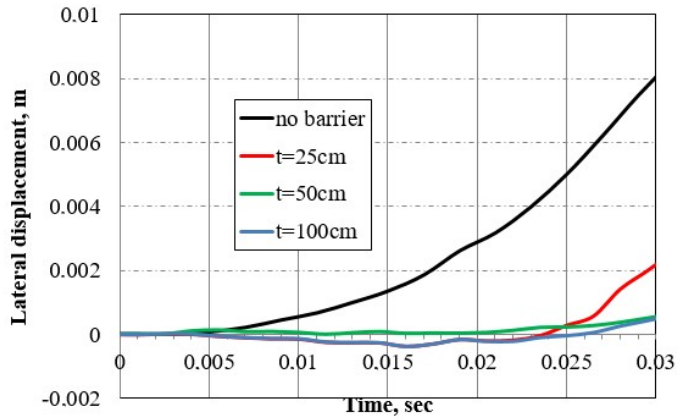

Figure 22. Lateral displacement at central of Pile No. 4.

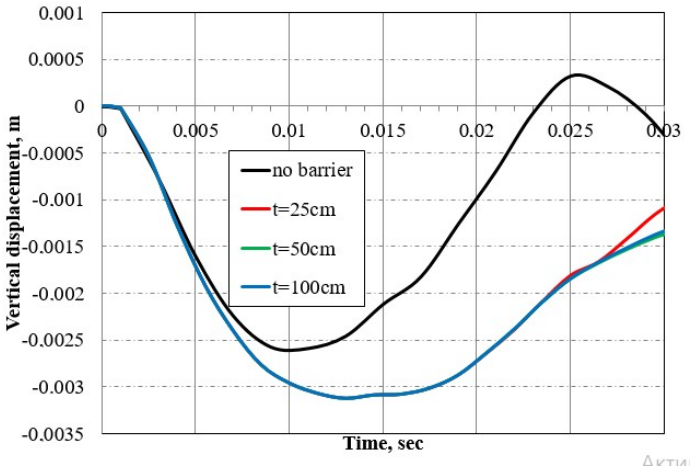

Figure 23. Vertical displacement at central of Pile No. 4.

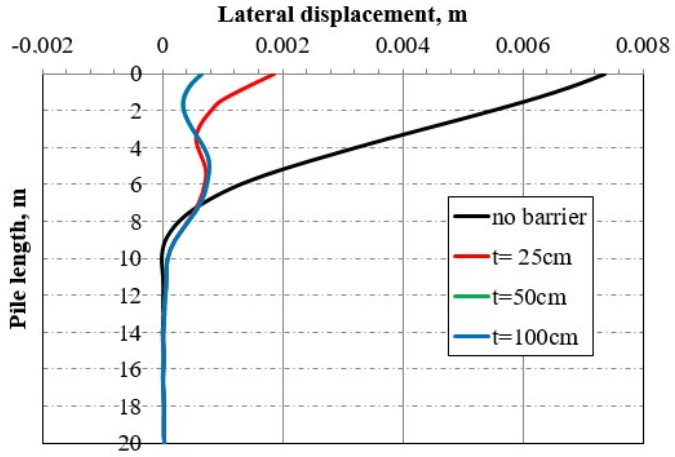

Figure 24. Lateral displacement at central of Pile No. 5 at *t* = 0.03 seconds.

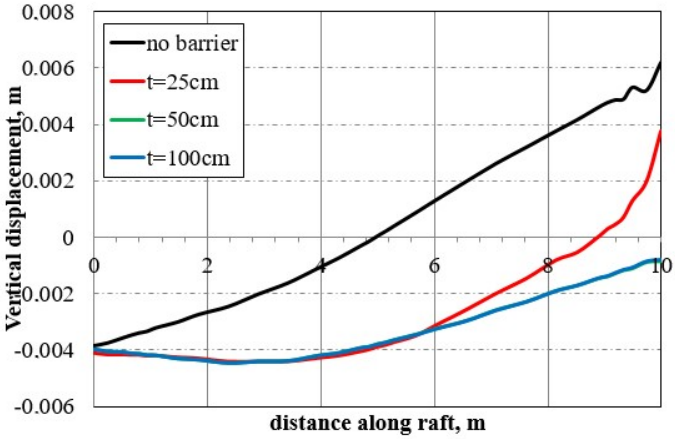

Figure 25. Vertical displacement along line BE at raft at *t* = 0.03 seconds.

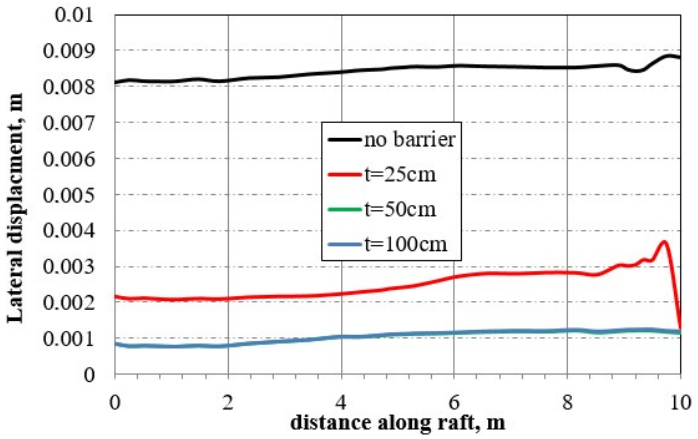

Figure 26. Lateral displacement along line BE at raft.

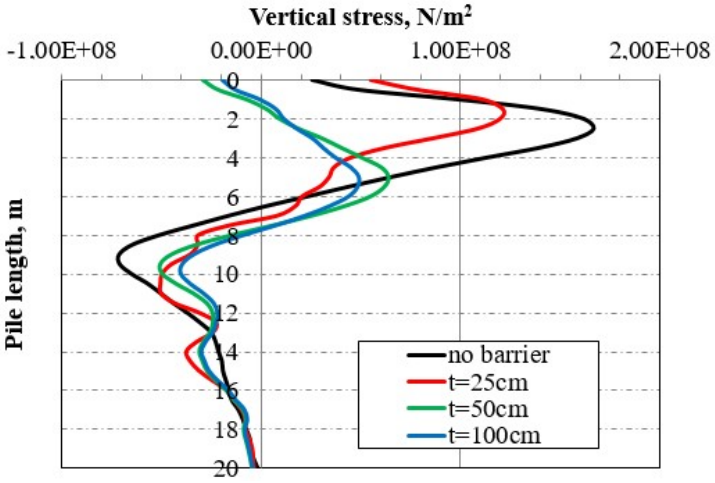

Figure 27. Vertical stress along Pile No. 4.

On the other hand, it might be considered to increase the depth of the wall barrier to provide better protection for the pile foundation system. The original case considered had wall barrier with a total depth of 5.0 m. Most of the large deformations obtained in piles were observed in top 5.0 m of the pile length. Accordingly, another parametric study was conducted to investigate the effect of having different depths of wall barrier including 10.0 and 15.0 m and the results were compared to the case considered earlier (depth of 5.0 m) and the original case that had no wall barrier. The results are shown in Figures 28 to 31. According to the results obtained, increasing the wall depth had no significant enhancement on the pile and foundation performance under blast load. There was no considerable protection obtained upon increasing the depth of the wall barrier to 10.0 or 15.0 m against the surface blast load. A depth of 5.0 m of EPS wall barrier was considered the optimal wall barrier in all cases considered.

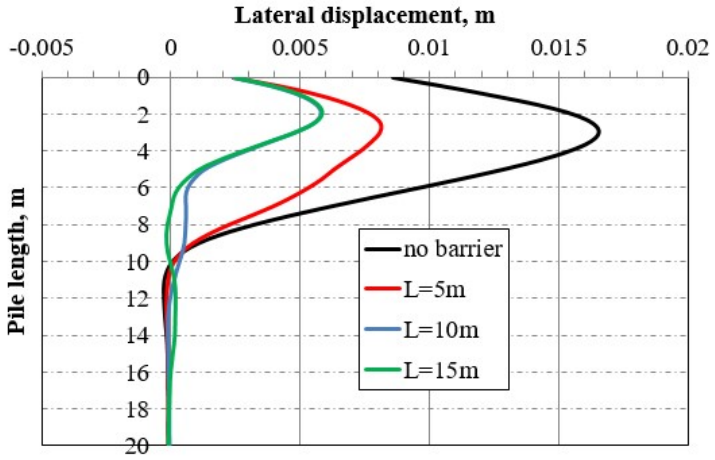

Figure 28. Lateral displacement of Pile No. 4 at *t* = 0.03 seconds.

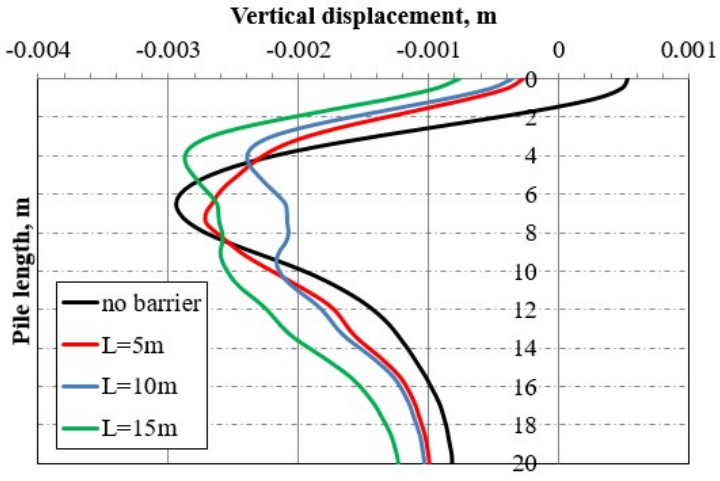

Figure 29. Vertical displacement of Pile No. 4 at *t* = 0.03 seconds.

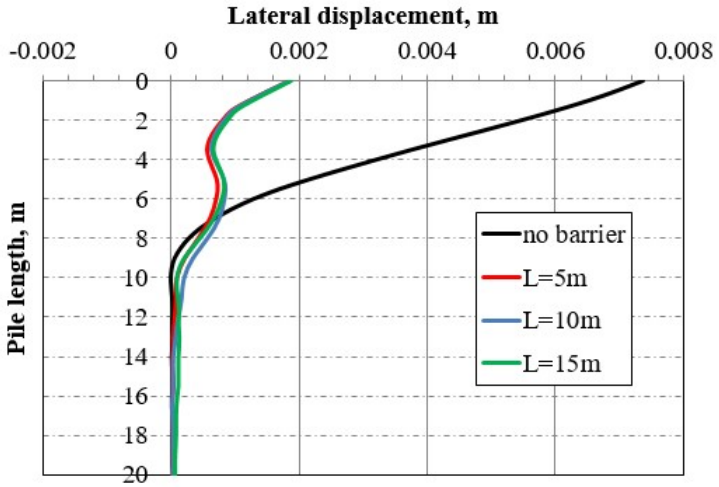

Figure 30. Lateral displacement of Pile No. 5 over its length at *t* = 0.03 seconds.

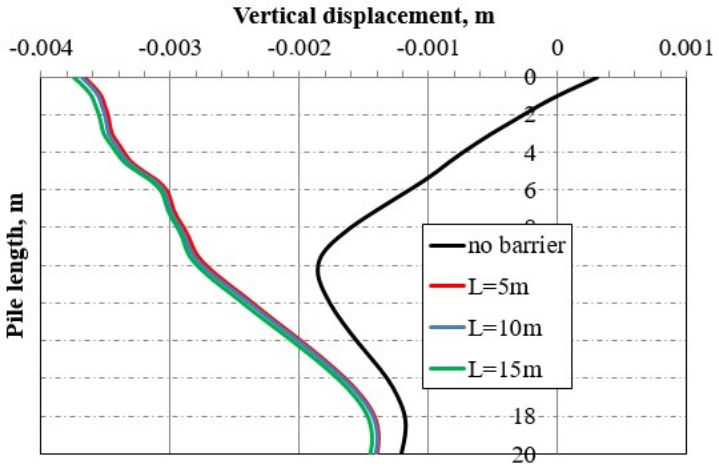

Figure 31. Vertical displacement of Pile No. 5 over its length at *t* = 0.03 seconds.

4. Conclusions

A finite element analysis using ABAQUS was conducted to study the effect of surface blast load on pile foundation considering different techniques in order to reduce the risk of the blast load. The pile foundation system consisted of nine 20-m length concrete piles encased in steel pipes with external diameter of 0.6 m and connected with a raft foundation of 10.0×10.0 m in plane dimensions and a thickness of 1.0 m. The soil profile consisted of upper layer of silty clay with a total thickness of 10 m. This layer was followed by 40-m thick stiff clay. The raft was loaded by 200 kN/m^2 to represent the load transferred from the structure. Explosive charge of 457 kg of TNT was assumed at a standoff distance 2.5 m from raft and at a height of 0.56 m above ground surface. Different techniques were considered in the study including using open trench before the pile foundation and wall barrier from different materials with a dimension of 10.0 m length, 0.25 m thickness and a

depth of 5.0 m with its top at the ground surface. According to the results, the following conclusions were obtained:

1. The open trench provides significant protection to the pile foundations under blast load effect. The enhancement in the response of the pile foundation upon using the open trench was better than all the wall barriers used.

2. Wall barriers can provide good enhancement of response of soil and pile foundation against surface blast load. However, the material of the wall barrier can play a vital role in this effect. Expanded Polystyrene (EPS) was the best material used for the wall barrier due to its hyperelastic and viscoelastic properties.

3. The protection provided by the wall barrier to the pile foundation against surface blast load is significantly affected by the thickness of the wall barrier. Larger thickness of wall barrier provides better enhancement and protection to the pile foundation. However, this should be considered with the cost of the wall barrier and the importance of the building and how susceptible to possible terrorist attack.

4. A depth of 5.0 m is sufficient for the wall barrier to provide significant protection to surface blast load threat. Larger depths provide slight enhancement that is not worthy compared to the increase in cost and construction challenges.

The study will be extended to investigate if similar results can be obtained when considering the effect of surface blast load on underground structures considering different parameters as the depth of underground structure, soil profile and various possible mitigation techniques.

5. Acknowledgement

The authors would like to express their thanks to Prince Sultan University for supporting in publishing the article.

References

1. Ismail, M., Ibrahim, Y., Nabil, M., Ismail, M.M. Response of A 3-D reinforced concrete structure to blast loading. International Journal of Advanced and Applied Sciences. 2017. 4. 10. Pp. 46–53.
2. Ibrahim, Y.E., Ismail, M.A., Nabil, M.A. Response of Reinforced Concrete Frame Structures under Blast Loading. Procedia Engineering. 2017. 171. Pp. 890–898.
3. Fu, F. Dynamic response and robustness of tall buildings under blast loading, Journal of Constructional Steel Research. 2013. 80. Pp. 299–307.
4. Choi, J., Choi, S., Kim, J. J. and Hong, K. Evaluation of blast resistance and failure behaviour of prestressed concrete under blast loading. Construction and Building Materials. 2018. 173. Pp. 550–572.
5. Ritchie, C.B., Packer, J.A., Seica, M.V., Zhao. X. Behaviour and analysis of concrete-filled rectangular hollow sections subject to blast loading. Journal of Constructional Steel Research. 2018. 147. Pp. 340–359.
6. Hadianfard, M.A., Malekpour, S., Momeni, M. Reliability analysis of H-section steel columns under blast loading, Structural Safety. 2018. 75. Pp. 45–56.
7. Baker, W.E. Explosions in Air. Austin. 1973. Texas, University of Texas Press.
8. ASCE. Manual 42, Design of Structures to Resist Nuclear Weapons Effects. New York City, New York. American Society of Civil Engineers, 1985.
9. Cooper, P.W. Explosives Engineering. Hoboken, New Jersey: John Wiley & Sons, Inc., 1996.
10. ABAQUS 6.14 User Documentation. Dessault Systems, 2018.
11. ANSYS. AUTODYN User's Manual. Canonsburg, Pennsylvania: ANSYS Inc., 2018.
12. LS-DYNA User's Manual. Livermore Software Technology Corporation, 2018.
13. Lu, Y. Underground blast induced ground shock and its modeling using artificial neural network. Computers and Geotechnics, 2005. 32. Pp. 164–178.
14. Gui, M.W., Chien, M.C. Blast-resistant analysis for a tunnel passing beneath Taipei Shongsan airport–a parametric study. Geotechnical & Geological Engineering. 2006. 24. Pp. 227–248.
15. Wang, J.G., Sun, W., Anand, S. Numerical investigation on active isolation of ground shock by soft porous layers. Journal of Sound and Vibration. 2009. 321. Pp. 492–509.
16. Shin, J.H., Moon, H.G., Chae, S.E. Effect of blast-induced vibration on exiting tunnels in soft rocks. Tunnelling and Underground Space Technology. 2011. 26. Pp. 51–61.
17. Feldgun, V.R., Karinski, Y.S., Yankelevsky, D.Z. The effect of an explosion in a tunnel on a neighboring buried structure. Tunnelling and Underground Space Technology. 2014. 44. Pp. 42–55.
18. De, A., Morgante, N., Zimmie, T.F. Numerical and physical modeling of geofoam barriers as protection against effects of surface blast on underground tunnels, Geotextiles and Geomembranes. 2016. 44. Pp. 1–12.
19. DOD. Structures to Resist the Effects of Accidental Explosions. Unified Facilities Criteria (UFC) 3–340–02. Arlington, Virginia: Department of Defense, 2008.
20. Zhang, Y, Chen, Y., Chen, S., Liu, H., Fu, Z. Experimental study on deformation of a sandy field liquefied by blasting. Soil Dynamics and Earthquake Engineering. 2019. 116. Pp. 60–68.
21. DOD. Fundamentals of Protective Design for Conventional Weapons. TM 5–855–1. Arlington, Virginia. Department of Defense, 1986.

22. Larcher, M. Simulation of the Effects of an Air Blast Wave. JRC Technical Notes (JRC) 41337. Luxembourg: European Communities, 2007.
23. Kinney, G.F., Graham, K.J. Explosive Shocks in Air. Berlin, Germany: Springer-Verlag, 1985.
24. Krauthammer, T., Altenberg. A. Negative Phase Blast Effects on Glass Panels. International Journal of Impact Engineering. 2000. 24. Pp. 1–17.
25. Smith, P.D., Hetherington, J.G. Blast and Ballistic Loading of Structures. Oxford, England: Butterworth-Heinemann, 1994.
26. Wang, Z., Lu, Y., Bai, C. Numerical Analysis of Blast-Induced Liquefaction of Soil. Computers and Geotechnics. 2008. 35. 2. Pp. 196–209.
27. Ibrahim, Y, Nabil, M. Finite Element Analysis of Pile Foundations under Surface Blast Loads. 13th International Conference on Damage Assessment of Structures. Porto, Portugal, 2019. July 9–10.
28. Davies, M.C.R. Dynamic soil structure interaction resulting from blast loading. Proceeding of the International Conference on Centrifuge Modelling (Centrifuge 94). Singapore, 1994. Pp. 319—324.
29. De, A., Morgante, A.N., Zimmie, T.F. Numerical and physical modeling of geofoam barriers as protection against effects of surface blast on underground tunnels. Geotextiles and Geomembranes. 2016. 44. Pp. 1–12.
30. De, A., Zimmie, T.F Centrifuge modeling of surface blast effects on underground structures Geotechnical Testing Journal. 2007. 30. Pp. 88–93.
31. Baziar, M.H., Shahnazari, H. Kazemi, H. Mitigation of surface impact loading effects on the underground structures with geofoam barrier: Centrifuge modeling. Tunneling and Underground Space Technology. 2018. 80. Pp. 128–142.
32. Gould, K.E. High explosive field tests: Explosion Phenomena and Environmental Impacts, DNA 6187F. 1981. Washington, DC: Defense Nuclear Agency.
33. NUREG/CR-7201: Characterizing Explosive, Effects on Underground Structures, Center for Nuclear Waste Regulatory Analyses. 2015. U.S. Nuclear Regulatory Commission Washington, DC 20555–0001.
34. Nagy, N., Mohamed, M., Boot, J.C. Nonlinear Numerical Modelling for the Effects of Surface Explosions on Buried Reinforced Concrete Structures. Geomechanics and Engineering. 2010. 2. Pp. 1–18.
35. Huang, T.K., Chen. W.F. Simple Procedure for Determining Cap-Plasticity-Model Parameters. Journal of Geotechnical Engineering. 1990. 116. 3. Pp. 492–513.
36. Chopra, A.K., Chakrabarti, P. The Koyna Earthquake and the Damage to the Koyna Dam, Bulletin of Seismological Society of America. 1973. 63. 2. Pp. 381–397.
37. Martin, O. Comparison of different Constitutive Models for Concrete in ABAQUS/Explicit for Missile Impact Analyses. JRC Scientific and Technical Reports. EUR 24151. European Commission, Joint Research Centre, Institute for Energy, 2010.
38. Johnson, G.R., Cook, W.H. Fracture characteristics of three metals subjected to various strains, strain rates, temperatures and pressures. Engineering Fracture Mechanics. 1985. 21. Pp. 31–48.
39. Jamil, Z.W., Guan, W.J., Cantwell, X.F., Zhang, G.S., Langdon G.S., Wang, Q.Y. Blast response of aluminum/thermoplastic polyurethane sandwich panels – experimental work and numerical analysis. International Journal of Impact Engineering. 2019. 127. Pp. 31–40.
40. Dassault Systems. ABAQUS/Standard; Theory Manual and Example Problems Manual; Release 6.12. Dassault Systems. Waltham, MA, USA, 2011.

Contacts:

Yasser Ibrahim, 00966553470474; yibrahim@vt.edu
Marwa Nabil, +201222694682; marwa_nabil_amin@yahoo.com

: